Chapter 7
Electrocatalytic Reactions Involving Hydrogen

Many reactions of industrial importance are electrocatalytic, i.e., they involve the specific adsorption of intermediates, for example hydrogen, chlorine, and oxygen evolution, oxygen reduction, and methanol or ethanol oxidation in fuel cells. Many different electrochemical techniques were used to study these reactions, and EIS is one of them, providing interesting kinetic and surface information. Certain model reactions will be presented in what follows with a detailed method of relating impedance parameters with mechanistic and kinetic equations.

7.1 Hydrogen Underpotential Deposition Reaction

On several noble metals (Pt, Rh, Ru, Ir, and Pd) hydrogen adsorption takes place at the potentials positive to the equilibrium potential for the hydrogen evolution reaction. This is a so-called hydrogen underpotential deposition reaction (HUPD) and indicates a strong adsorptive interaction between atomic hydrogen and the surface metal atoms. Similar UPD processes are observed for the deposition of metals on metals [237]. Certain reactions, like Cu UPD at Pt, Ru, or Rh, are used as diagnostic tools to determine the real surface area of electrocatalytic materials.

Although the adsorption isotherms are usually complex [238], the simplest Langmuir isotherm will be presented first and later the Frumkin isotherm will be shown. The following development is similar to that in Sect. 5.1. The HUPD reaction in acid and alkaline solutions may be written as

$$\mathrm{H^+ + M} + e \underset{\overleftarrow{k}_{-1}}{\overset{\overrightarrow{k}_1}{\rightleftharpoons}} \mathrm{MH_{ads}} \tag{7.1}$$

A. Lasia, *Electrochemical Impedance Spectroscopy and its Applications*,
DOI 10.1007/978-1-4614-8933-7_7, © Springer Science+Business Media New York 2014

or

$$\mathrm{H_2O} + \mathrm{M} + e \underset{\overleftarrow{k}_{-1}}{\overset{\overrightarrow{k}_1}{\rightleftharpoons}} \mathrm{MH_{ads}} + \mathrm{OH^-}. \tag{7.2}$$

The kinetic equations in acid solution are

$$i = -Fv_1 = \frac{\mathrm{d}Q}{\mathrm{d}t} = -F\frac{\mathrm{d}\Gamma_\mathrm{H}}{\mathrm{d}t} = -\sigma_1\frac{\mathrm{d}\theta_\mathrm{H}}{\mathrm{d}t}, \tag{7.3}$$

$$\begin{aligned} v_1 &= k_1^0 C_{\mathrm{H^+}}(0)(\Gamma_\infty - \Gamma_H)e^{-\beta f\left(E-E_1^0\right)} - k_{-1}^0\Gamma_\mathrm{H}\mathrm{e}^{(1-\beta)f\left(E-E_1^0\right)} \\ &= \Gamma_\infty\left[k_1^0 C_{\mathrm{H^+}}(0)(1-\theta_\mathrm{H})\mathrm{e}^{-\beta f\left(E-E_1^0\right)} - k_{-1}^0\theta_\mathrm{H}\mathrm{e}^{(1-\beta)f\left(E-E_1^0\right)}\right], \end{aligned} \tag{7.4}$$

where Q is the charge corresponding to the adsorption of H (C cm^{-2}), v_1 is the reaction rate (mol cm^{-2} s^{-1}), $\sigma_1 = F\,\Gamma_\mathrm{H}$ is the charge necessary for one monolayer coverage by adsorbed H (C cm^{-2}), k_1^0 is the standard rate constant of hydrogen adsorption (cm^3 mol^{-1} s^{-1}), k_{-1}^0 is the standard rate constant of desorption (s^{-1}), $C_{\mathrm{H^+}}(0)$ is the surface concentration of hydrogen ions, Γ_∞ is the total surface concentration of adsorption sites (mol cm^{-2}), Γ_H is the surface concentration of adsorbed H, E_1^0 is the standard potential of reaction (7.1), θ_H is the fractional surface coverage by adsorbed hydrogen, and $\theta_\mathrm{H} = \Gamma_\mathrm{H}/\Gamma_\infty$. It is evident that the current can flow only when there is a change in surface coverage and in the steady state the current is zero. The equilibrium and peak potential for the HUPD reaction are described by (5.4) and (5.5).

Assuming that the bulk and surface concentrations are the same (i.e., the hydrogen surface concentration is not affected by the passing current) the following equation is obtained:

$$\begin{aligned} v_1 &= \Gamma_\infty\left(k_1^0\right)^{1-\beta}\left(k_{-1}^0\right)^{\beta}\left(C_{\mathrm{H^+}}^*\right)^{1-\beta}(1-\theta_\mathrm{H})\mathrm{e}^{-\beta f\left(E-E_\mathrm{p}\right)} \\ &\quad - \Gamma_\infty\left(k_1^0\right)^{1-\beta}\left(k_{-1}^0\right)^{\beta}\left(C_{\mathrm{H^+}}^*\right)^{1-\beta}\theta_\mathrm{H}\mathrm{e}^{(1-\beta)f\left(E-E_\mathrm{p}\right)} \\ &= k^0\mathrm{e}^{-\beta f\left(E-E_\mathrm{p}\right)}(1-\theta_\mathrm{H}) - k^0\mathrm{e}^{(1-\beta)f\left(E-E_\mathrm{p}\right)}\theta_\mathrm{H} \\ &= \overrightarrow{k}_1(1-\theta_\mathrm{H}) - \overleftarrow{k}_1\theta_\mathrm{H}, \end{aligned} \tag{7.5}$$

where $k^0 = \Gamma_\infty\left(k_1^0\right)^{1-\beta}\left(k_{-1}^0\right)^{\beta}\left(C_{\mathrm{H^+}}^*\right)^{1-\beta}$ is the concentration-dependent rate constant, and the potential-dependent rate constants are $\overrightarrow{k}_1 = k^0\exp\left[-\beta f\left(E-E_\mathrm{p}\right)\right]$ and $\overleftarrow{k}_1 = k^0\exp\left[(1-\beta)f\left(E-E_\mathrm{p}\right)\right]$. For simplicity let us introduce the overpotential $\eta = E - E_\mathrm{p}$, see Eq. (5.5). The further development is identical to that described in Sect. 5.1 [61, 211]. The faradaic impedance is described in Eq. (5.19) and the dependence of the parameters R_ct and C_p on the potential is shown in Fig. 5.1. At the current peak potential the charge transfer resistance is at a minimum and the pseudocapacitance at a maximum. It is interesting to note that for the Langmuir

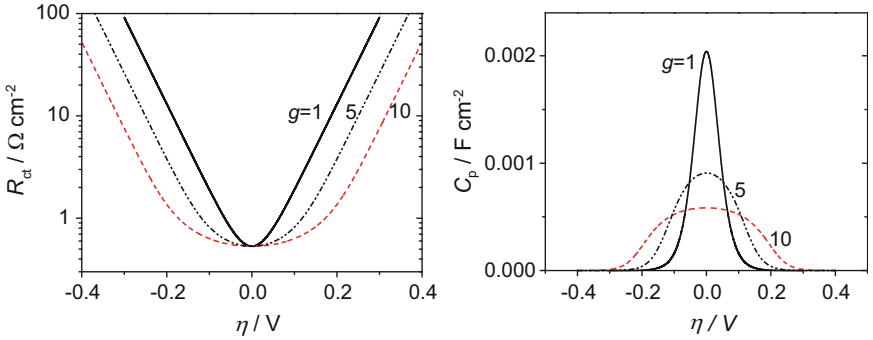

Fig. 7.1 Comparison of parameters R_{ct} and C_p for HUPD reaction, continuous line Langmuir isotherm, $g = 1$, *dash-dotted* and *dashed lines*: Frumkin isotherm with $g = 5$ and 10, $k^0 = 10^{-6}$ mol cm^{-2} s^{-1}

adsorption isotherm the maximum value of the pseudocapacitance, C_p, depends only on the total hydrogen adsorption charge, $\sigma_1 = 210\ \mu C\ cm^{-2}$ [239], and equals 2.04 mF cm^{-2}.

In the case of the Frumkin adsorption isotherm, which includes lateral interactions between adsorbed hydrogen atoms, the reaction rate is described by [240]

$$\begin{aligned} v_1 &= k^0 \exp(-\beta f\eta)\exp[-\lambda g(\theta_H - 0.5)](1-\theta_H) \\ &\quad - k^0 \exp[(1-\beta)f\eta]\exp[(1-\lambda)g(\theta_H - 0.5)]\theta_H \\ &= \vec{k}_1 \exp[-\lambda g(\theta_H - 0.5)](1-\theta_H) - \overleftarrow{k}_1 \exp[(1-\lambda)g(\theta_H - 0.5)]\theta_H, \end{aligned} \tag{7.6}$$

where g is the interaction parameter, positive for repulsions and negative for interactions [17], and λ is the adsorption symmetry factor between 0 and 1, typically ~0.5 [240]. In the steady state, the current is equal to zero and the following relation is obtained:

$$\frac{\theta_H}{1-\theta_H} e^{g(\theta_H - 0.5)} = e^{-f\eta}, \tag{7.7}$$

which is the definition of the Frumkin isotherm. Continuing the development, the same expression for the impedance is obtained, Eq. (5.19), but with different values of the derivatives $\partial v_1/\partial\eta$ and $\partial v_1/\partial\theta_H$. The influence of the parameter g on the parameters R_{ct} and C_p is illustrated in Fig. 7.1.

It is evident that an increase in the repulsion between H atoms causes a flattening of both curves and a decrease in the maximum of the pseudocapacitance. It can be added that the Frumkin isotherm was found to describe HUPD at Pt(100) in $HClO_4$, Pt(110) in H_2SO_4, and Pt(111) in both acids [241]. The value of the parameter g at Pt(111) was approximately 12. Unfortunately, the isotherms at other surfaces or metals are much more complicated. The HUPD kinetics was studied on different polycrystalline metals. It was found that the kinetics at Pt [242] was about three orders of magnitude faster than that at Ru [243], Pd [244, 245], or Rh [246] electrodes, while that at Ir was intermediate between those groups [247] (on the

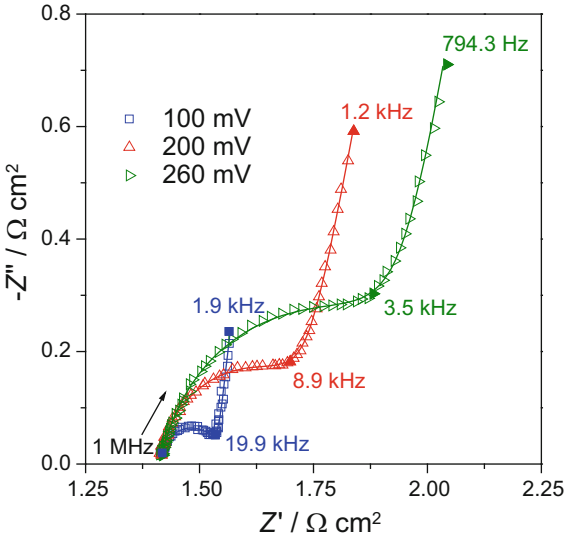

Fig. 7.2 Complex plane plots for HUPD reaction at polycrystalline Pt electrode in 0.1 M H_2SO_4; potentials versus reversible hydrogen electrode indicated in graph. *Points* – experimental, *lines* – fit (From Ref. [242], copyright (2012), with permission from Elsevier)

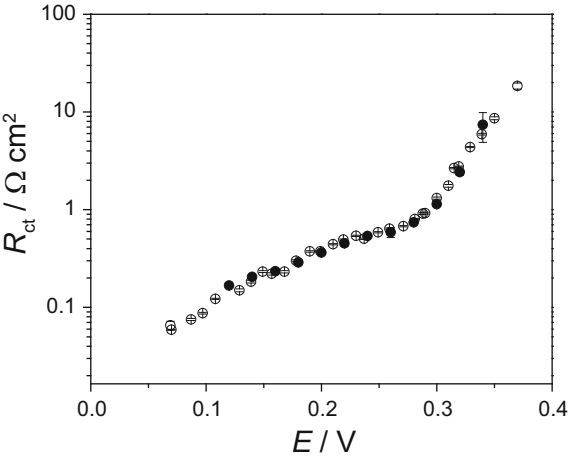

Fig. 7.3 Dependence of charge transfer resistance (per real surface area) on potential for HUPD reaction at polycrystalline Pt in 0.1 M H_2SO_4 (From Ref. [242], copyright (2012), with permission from Elsevier)

logarithmic scale). An example of the complex plane plots obtained at polycrystalline Pt in H_2SO_4 is presented in Fig. 7.2. To approximate the experimental curves, it was necessary to replace C_{dl} and C_p by the constant phase elements, CPE, see Chap. 8. The dependence of the charge transfer resistance on the potential is shown in Fig. 7.3.

It is evident that R_{ct} decreases with a decrease in the electrode potential in the entire range. At the lowest potentials there is an influence of the overpotentially deposited hydrogen (HOPD), which is related to the classical hydrogen evolution, and dissolved hydrogen formation at the solution around the electrode. The kinetics is very fast and was measured without a potentiostat [242]. Because the adsorption isotherm is rather complex [248] no rate constants were determined. It should be added that in earlier studies, at monocrystalline Pt, it was found that R_{ct} was potential independent [249], which may be connected with equipment artifacts.

7.2 Hydrogen Evolution Reaction

The hydrogen evolution reaction (HER) is one of the most important and most studied electrocatalytic processes [61, 211, 239, 250, 251]. It is well accepted that the first step is the Volmer reaction, (7.8), followed by Heyrovsky, (7.9), or Tafel, (7.10), steps. Because the process is usually carried out in alkaline solutions these steps are written as follows:

$$\mathrm{H_2O} + \mathrm{M} + e \underset{\overleftarrow{k}_{-1}}{\overset{\vec{k}_1}{\rightleftharpoons}} \mathrm{MH_{ads}} + \mathrm{OH^-}, \tag{7.8}$$

$$\mathrm{MH} + \mathrm{H_2O} + e \underset{\overleftarrow{k}_{-2}}{\overset{\vec{k}_2}{\rightleftharpoons}} \mathrm{M} + \mathrm{OH^-} + \mathrm{H_2}, \tag{7.9}$$

$$2\mathrm{MH} \underset{k_{-3}}{\overset{k_3}{\rightleftharpoons}} 2\mathrm{M} + \mathrm{H_2}. \tag{7.10}$$

It might be noticed that the Volmer and Heyrovsky reactions are electrochemical while the Tafel reaction is chemical, without an exchange of electrons. Assuming a Langmuir adsorption isotherm for H, the rates, ν_i, are written as

$$v_1 = k_1^0 \Gamma_\infty a_{\mathrm{H_2O}} (1-\theta_\mathrm{H}) \mathrm{e}^{-\beta_1 f\left(E-E_1^0\right)} - k_{-1}^0 \Gamma_\infty a_{\mathrm{OH^-}} \theta_\mathrm{H} \mathrm{e}^{(1-\beta_1) f\left(E-E_1^0\right)}, \tag{7.11}$$

$$\begin{aligned} v_2 = {} & k_2^0 \Gamma_\infty a_{\mathrm{H_2O}} \theta_\mathrm{H} \mathrm{e}^{-\beta_2 f\left(E-E_2^0\right)} \\ & - k_{-2}^0 \Gamma_\infty a_{\mathrm{H_2}} a_{\mathrm{OH^-}} (1-\theta_\mathrm{H}) \mathrm{e}^{(1-\beta_2) f\left(E-E_2^0\right)}, \end{aligned} \tag{7.12}$$

$$v_3 = \left(k_3^0 \Gamma_\infty^2\right) \theta_\mathrm{H}^2 - \left(k_{-3}^0 \Gamma_\infty^2\right) (1-\theta_\mathrm{H})^2 a_{\mathrm{H_2}}. \tag{7.13}$$

For simplicity the surface concentrations of $\mathrm{OH^-}$, $\mathrm{H_2O}$, and $\mathrm{H_2}$ are written as dimensionless $a_\mathrm{i} = C_\mathrm{i}(0)/C^*$, where the superscripted asterisk denotes bulk or equilibrium values. In general, the standard potentials of the Volmer and Heyrovsky steps are different. Proceeding in a way similar to that described in Sect. 5.2.1 the following equations are obtained:

$$\begin{aligned} v_1 = {} & \left\{ \left(k_1^0\right)^{(1-\beta_1)} \left(k_{-1}^0\right)^{\beta_1} \Gamma_\infty \left(\frac{a_{\mathrm{OH^-}}^*}{a_{\mathrm{H_2O}}^*} \frac{\theta_\mathrm{H}^*}{1-\theta_\mathrm{H}^*} \right)^{\beta_1} \right\} a_{\mathrm{H_2O}} (1-\theta_\mathrm{H}) \exp(-\beta_1 f\eta) \\ & - \left\{ \left(k_1^0\right)^{(1-\beta_1)} \left(k_{-1}^0\right)^{\beta_1} \Gamma_\infty \left(\frac{a_{\mathrm{H_2O}}^*}{a_{\mathrm{OH^-}}^*} \frac{1-\theta_\mathrm{H}^*}{\theta_\mathrm{H}^*} \right)^{1-\beta_1} \right\} a_{\mathrm{OH^-}} \theta_\mathrm{H} \exp[(1-\beta_1) f\eta], \end{aligned} \tag{7.14}$$

$$v_2 = \left\{ \left(k_2^0\right)^{(1-\beta_2)} \left(k_{-2}^0\right)^{\beta_2} \Gamma_\infty \left(\frac{a^*_{H_2} a^*_{OH^-}}{a^*_{H_2O}} \frac{1-\theta^*_H}{\theta^*_H} \right)^{\beta_2} \right\} a_{H_2O} \theta_H \exp(-\beta_2 f\eta)$$

$$- \left\{ \left(k_2^0\right)^{(1-\beta_2)} \left(k_{-2}^0\right)^{\beta_2} \Gamma_\infty \left(\frac{a^*_{H_2O}}{a^*_{H_2} a^*_{OH^-}} \frac{\theta^*_H}{1-\theta^*_H} \right)^{1-\beta_2} \right\} a_{H_2} a_{OH^-} (1-\theta_H) \exp[(1-\beta_2) f\eta]. \tag{7.15}$$

Assuming that the surface and bulk concentrations are the same one obtains

$$v_1 = k_1(1-\theta_H)e^{-\beta_1 f\eta} - k_{-1}\theta_H e^{(1-\beta_1)f\eta} = \vec{k}_1(1-\theta_H) - \overleftarrow{k}_{-1}\theta_H, \tag{7.16}$$

$$v_2 = k_2\theta_H e^{-\beta_2 f\eta} - k_{-2}(1-\theta_H)e^{(1-\beta_2)f\eta} = \vec{k}_2\theta_H - \overleftarrow{k}_{-2}(1-\theta_H), \tag{7.17}$$

$$v_3 = k_3\theta_H^2 - k_{-3}(1-\theta_H)^2, \tag{7.18}$$

where

$$k_1 = \left(k_1^0\right)^{(1-\beta_1)} \left(k_{-1}^0\right)^{\beta_1} \Gamma_\infty \left(\frac{a^*_{OH^-}}{a^*_{H_2O}} \frac{\theta^*_H}{1-\theta^*_H} \right)^{\beta_1},$$

$$k_{-1} = \left(k_1^0\right)^{(1-\beta_1)} \left(k_{-1}^0\right)^{\beta_1} \Gamma_\infty \left(\frac{a^*_{H_2O}}{a^*_{OH^-}} \frac{1-\theta^*_H}{\theta^*_H} \right)^{1-\beta_1}, \tag{7.19}$$

$$k_2 = \left(k_2^0\right)^{(1-\beta_2)} \left(k_{-2}^0\right)^{\beta_2} \Gamma_\infty \left(\frac{a^*_{H_2} a^*_{OH^-}}{a^*_{H_2O}} \frac{1-\theta^*_H}{\theta^*_H} \right)^{\beta_2},$$

$$k_{-2} = \left(k_2^0\right)^{(1-\beta_2)} \left(k_{-2}^0\right)^{\beta_2} \Gamma_\infty \left(\frac{a^*_{H_2O}}{a^*_{H_2} a^*_{OH^-}} \frac{\theta^*_H}{1-\theta^*_H} \right)^{1-\beta_2}, \tag{7.20}$$

$$k^3 = k_3^0 \Gamma_\infty^2,$$

$$k_{-3} = k_{-3}^0 \Gamma_\infty^2 a^*_{H_2}. \tag{7.21}$$

Equations (7.16), (7.17), and (7.18) can also be presented in another form:

$$v_1 = v_1^0 \left[\left(\frac{1-\theta_H}{1-\theta^*_H} \right) \left(\frac{a_{H_2O}}{a^*_{H_2O}} \right) \exp(-\beta_1 f\eta) - \left(\frac{\theta_H}{\theta^*_H} \right) \left(\frac{a_{OH^-}}{a^*_{OH^-}} \right) \exp[(1-\beta_1) f\eta] \right], \tag{7.22}$$

$$v_2 = v_2^0 \left[\begin{array}{l} \left(\frac{\theta_H}{\theta_H^0}\right)\left(\frac{a_{H_2O}}{a_{H_2O}^*}\right)\exp(-\beta_2 f\eta) \\ -\left(\frac{1-\theta_H}{1-\theta_H^0}\right)\left(\frac{a_{H_2}}{a_{H_2}^*}\right)\left(\frac{a_{OH^-}}{a_{OH^-}^*}\right)\exp[(1-\beta_2)f\eta] \end{array} \right], \tag{7.23}$$

$$v_3 = v_3^0 \left[\left(\frac{\theta_H}{\theta_H^*}\right)^2 - \left(\frac{1-\theta_H}{1-\theta_H^*}\right)^2 \left(\frac{a_{H_2}}{a_{H_2}^*}\right) \right], \tag{7.24}$$

where

$$v_1^0 = \left(k_1^0\right)^{(1-\beta_1)} \left(k_{-1}^0\right)^{\beta_1} \Gamma_\infty \left(a_{OH^-}^*\right)^{\beta_1} \left(a_{H_2O}^*\right)^{1-\beta_1} \left(\theta_H^*\right)^{\beta_1} \left(1-\theta_H^*\right)^{1-\beta_1}, \tag{7.25}$$

$$v_2^0 = \left(k_2^0\right)^{(1-\beta_2)} \left(k_{-2}^0\right)^{\beta_2} \Gamma_\infty \left(a_{H_2}^* a_{OH^-}^*\right)^{\beta_2} \left(a_{H_2O}^*\right)^{1-\beta_2} \left(\theta_H^*\right)^{1-\beta_2} \left(1-\theta_H^*\right)^{\beta_2}, \tag{7.26}$$

$$v_3^0 = \frac{k_3 k_{-3} \Gamma_\infty a_{H_2}^*}{\left(\sqrt{k_3} + \sqrt{k_{-3} a_{H_2}^*}\right)}. \tag{7.27}$$

It is important to remember that all rate constants, Eqs. (7.19), (7.20), and (7.21), and the standard rates, Eqs. (7.25), (7.26), and (7.27), are concentration dependent, and the experimenter should ensure that they stay constant at various current densities. It is also possible to redefine all the equations introducing the real surface concentrations, which should be known from the experiments. Then the current flowing in the system is described by

$$i = -F(v_1 + v_2) = -Fr_0. \tag{7.28}$$

At the equilibrium potential, the rates of all reactions are zero,

$$v_1 = v_2 = v_3 = 0, \tag{7.29}$$

and the following relation between the rate constants is obtained [217]:

$$\frac{k_1 k_2}{k_{-1} k_{-2}} = \frac{k_1^2 k_3}{k_{-1}^2 k_{-3}} = \frac{k_2^2 k_3}{k_{-2}^2 k_{-3}} = 1. \tag{7.30}$$

As a consequence, two equivalent solutions exist (see also Sect. 5.2.3) giving the same values of the physically measured currents and impedances [213–217] in which the appropriate rate constants can be exchanged:

$$k_1 \leftrightarrow k_2 \quad k_{-1} \leftrightarrow k_{-2} \quad k_3 \leftrightarrow k_{-3}. \tag{7.31}$$

The only difference is that the values of θ_H are replaced by $1–\theta_H$, that is, the surface coverage decreases or increases with the negative overpotential. This makes the rate constants indistinguishable, and other experiments must be used to decide which solution is correct.

At the steady state, the surface coverage by adsorbed hydrogen may be obtained from the condition that the rates of hydrogen adsorption and desorption are equal:

$$\frac{d\Gamma_H}{dt} = \frac{\sigma_1}{F}\frac{d\theta_H}{dt} = r_1 = v_1 - v_2 - 2v_3 = 0, \tag{7.32}$$

which leads to a second-order equation [217, 252, 253]. In the case where the Tafel reaction is neglected, a simpler equation is obtained:

$$\theta_H = \frac{\vec{k}_1 + \overleftarrow{k}_{-2}}{\vec{k}_1 + \overleftarrow{k}_{-1} + \vec{k}_2 + \overleftarrow{k}_{-2}}, \tag{7.33}$$

which, at negative overpotentials, reaches a constant value lower than unity (in contrast to the HUPD reaction):

$$\theta_H = \frac{k_1}{k_1 + k_2}, \tag{7.34}$$

Having described the HER in dc conditions the impedance of this process is described by the linearization of the changes in the surface coverage and the current:

$$\Delta i = \left(\frac{\partial i}{\partial \eta}\right)_{\theta_H} \Delta\eta + \left(\frac{\partial i}{\partial \theta_H}\right)_{\eta} \Delta\theta_H = F\left[\left(\frac{\partial r_0}{\partial \eta}\right)_{\theta_H} \Delta\eta + \left(\frac{\partial r_0}{\partial \theta_H}\right)_{\eta} \Delta\theta_H\right], \tag{7.35}$$

$$\frac{\sigma_1}{F}\frac{d\Delta\theta_H}{dt} = \Delta r_1 = \left(\frac{\partial r_1}{\partial \eta}\right)_{\theta_H} \Delta\eta + \left(\frac{\partial r_1}{\partial \theta_H}\right)_{\eta} \Delta\theta_H. \tag{7.36}$$

Following the procedure described in Sect. 5.2 the faradaic impedance described by Eq. (5.54) is obtained. The kinetics of the HER has been studied often using EIS, but the rate constants were rarely determined, e.g., at Ni [213, 254], Pt [255–258], alloys [259–262], or composite [263–269] electrodes. The best method for determining the rate constant is the simultaneous approximation of the impedance parameters and the dc current [213, 254, 263].

7.3 Influence of Hydrogen Mass Transfer on HER

During the HER, hydrogen is produced at the electrode surface, Eqs. (7.9), and (7.10), and diffuses toward the bulk of the solution. At the electrode surface at the rotating disk electrode (RDE), oversaturation may appear without bubble formation [180, 270, 271]. In such cases, reactions (7.12) and (7.13) should be rearranged to

$$v_2 = \vec{k}_2\theta_{\mathrm{H}} - \overleftarrow{k}_{-2}(1-\theta_{\mathrm{H}})a_{\mathrm{H}_2}, \tag{7.37}$$

$$v_3 = k_3\theta_{\mathrm{H}}^2 - k_{-3}(1-\theta_{\mathrm{H}})^2 a_{\mathrm{H}_2}, \tag{7.38}$$

where the definitions of k_2, k_{-2}, and k_{-3} must be modified to exclude the dimensionless surface concentration of hydrogen, a_{H_2}. Besides Eqs. (7.28), (7.29), (7.30), (7.31), and (7.32) another equation involving dissolved hydrogen flux, J_{H_2}, must be added:

$$J_{\mathrm{H}_2} = -D_{\mathrm{H}_2}C^0\frac{\mathrm{d}a_{\mathrm{H}_2}}{\mathrm{d}x} = v_2 + v_3 = r_2. \tag{7.39}$$

For the RDE one can write a simplified equation, $J_{\mathrm{H}_2} = D_{\mathrm{H}_2}C^0\left(a_{\mathrm{H}_2} - a^*_{\mathrm{H}_2}\right)/\delta$, where $\delta = 1.612D_{\mathrm{H}_2}^{1/3}\nu^{1/6}\Omega^{-1/2}$ and C^0 is the surface concentration of hydrogen (see also Sect. 4.9). Writing the equation for the flux phasor in finite-length transmissive mass transfer, Eq. (4.68), leads to

$$\widetilde{J}_{\mathrm{H}_2} = \widetilde{a}_{\mathrm{H}_2}\left[C^0\sqrt{j\omega D_{\mathrm{H}_2}}\coth\left(\sqrt{\frac{j\omega}{D_{\mathrm{H}_2}}}\delta\right)\right] = J'\widetilde{a}_{\mathrm{H}_2}. \tag{7.40}$$

The linearized equations describing the system are

$$\widetilde{i} = -F\left[\left(\frac{\partial r_0}{\partial\eta}\right)\widetilde{\eta} + \left(\frac{\partial r_0}{\partial\theta_{\mathrm{H}}}\right)\widetilde{\theta}_{\mathrm{H}}\right], \tag{7.41}$$

$$j\omega\frac{\sigma_1}{F}\widetilde{\theta}_{\mathrm{H}} = \left(\frac{\partial r_1}{\partial\eta}\right)\widetilde{\eta} + \left(\frac{\partial r_1}{\partial\theta_{\mathrm{H}}}\right)\widetilde{\theta}_{\mathrm{H}} + \left(\frac{\partial r_1}{\partial a_{\mathrm{H}_2}}\right)\widetilde{a}_{\mathrm{H}_2}, \tag{7.42}$$

$$J'\widetilde{a}_{\mathrm{H}_2} = \left(\frac{\partial r_2}{\partial\theta_{\mathrm{H}}}\right)\widetilde{\theta}_{\mathrm{H}} + \left(\frac{\partial r_2}{\partial a_{\mathrm{H}_2}}\right)\widetilde{a}_{\mathrm{H}_2}. \tag{7.43}$$

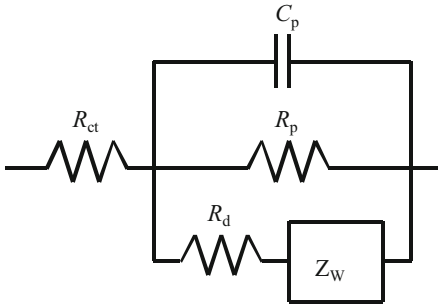

Fig. 7.4 Electrical equivalent circuit of faradaic impedance corresponding to HER with hydrogen diffusion, Eq. (7.48)

They may be written in matrix form:

$$\begin{bmatrix} -\dfrac{\partial r_0}{\partial \eta} \\ -\dfrac{\partial r_1}{\partial \eta} \\ 0 \end{bmatrix} = \begin{bmatrix} \dfrac{1}{F} & \dfrac{\partial r_0}{\partial \theta_H} & 0 \\ 0 & \dfrac{\partial r_1}{\partial \theta_H} - j\omega\dfrac{\sigma_1}{F} & \dfrac{\partial r_1}{\partial a_{H_2}} \\ 0 & \dfrac{\partial r_2}{\partial \theta_H} & \dfrac{\partial r_2}{\partial a_{H_2}} - J' \end{bmatrix} \begin{bmatrix} \dfrac{\widetilde{i}}{\widetilde{\eta}} \\ \dfrac{\widetilde{\theta}_H}{\widetilde{\eta}} \\ \dfrac{\widetilde{a}_{H_2}}{\widetilde{\eta}} \end{bmatrix}. \tag{7.44}$$

The faradaic admittance is

$$\hat{Y}_f = \frac{\widetilde{i}}{\widetilde{\eta}} = A + \frac{B}{j\omega + C + \dfrac{D}{E - J'}}, \tag{7.45}$$

where parameters A, B, and C are as defined in Eq. (5.52) and

$$D = \frac{F}{\sigma_1}\left(\frac{\partial r_1}{\partial a_{H_2}}\right)\left(\frac{\partial r_2}{\partial \theta_H}\right) \text{ and } E = \left(\frac{\partial r_2}{\partial a_{H_2}}\right). \tag{7.46}$$

The faradaic admittance may be rearranged into impedance:

$$\hat{Z}_f = R_{ct} + \frac{1}{j\omega C_p + \dfrac{1}{R_p} + \dfrac{1}{R_d + \hat{Z}_W}}, \tag{7.47}$$

where

$$R_d = -\frac{BE}{A^2 D}, \quad \hat{Z}_W = \frac{B}{A^2 D} C^0 \sqrt{j\omega D_{H_2}} \coth\left(\sqrt{\frac{j\omega}{D_{H_2}}}\delta\right). \tag{7.48}$$

The electrical equivalent circuit corresponding to Eq. (7.48) is presented in Fig. 7.4.

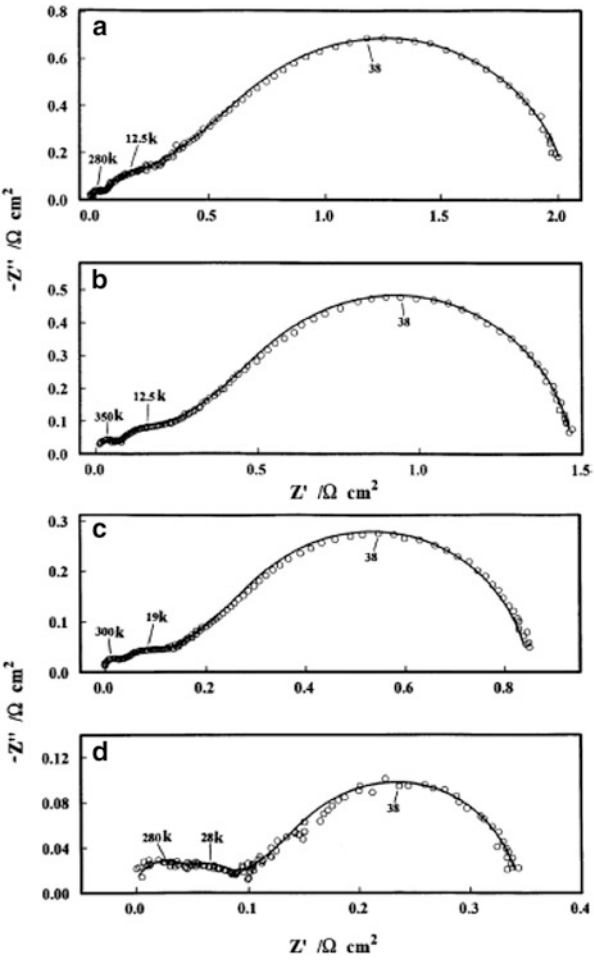

Fig. 7.5 Complex plane plots for Pt(511) at η (**a**) −7.3 mV; (**b**) −14 mV; (**c**) −30 mV; (**d**) −40 mV, in 0.5 M H_2SO_4 at RDE 3,500 rpm (From Ref. [180], copyright (1998), with permission from Elsevier)

Comparing this circuit with that for a simple hydrogen evolution without mass transfer effects, Fig. 5.1 left, it is evident that a new branch in parallel consisting of the resistance R_d in series with the finite-length mass transfer impedance, Z_w, was added to the circuit. Studies of the HER at various monocrystalline Pt surfaces displayed one or two semicircles followed by a finite-length diffusion impedance on the complex plane plots [180]. Examples of the impedance plots obtained at the rotating disk at the Pt(511) electrode are displayed in Fig. 7.5. The equations developed earlier might also be used to describe a hydrogen oxidation reaction.

7.4 Hydrogen Absorption into Metals

Besides hydrogen adsorption and evolution, hydrogen absorption into metals might occur. It is observed in Pd and certain alloys of the type AB_5 (e.g., $LaNi_5$) or AB_2 and is used in metal hydride batteries. The theory developed here is also applicable to other reactions, e.g., Li intercalation in Li-ion batteries. Let us consider first the simplest adsorption–absorption reaction [272].

7.4.1 Hydrogen Adsorption–Absorption Reaction in Presence of Hydrogen Evolution

In this case, the hydrogen adsorption reaction, (7.49), is followed by hydrogen evolution, (7.50) and (7.51), in parallel with hydrogen absorption, (7.52), during which a hydrogen atom at the surface goes to a subsurface site at a distance $x = 0$ [273–275]:

$$\mathrm{H^+} + e + \mathrm{M_{surface}} \underset{\overleftarrow{k}_{-1}}{\overset{\overrightarrow{k}_1}{\rightleftharpoons}} \mathrm{MH_{ads}}, \tag{7.49}$$

$$\mathrm{MH_{ads}} + \mathrm{H^+} + e \underset{\overleftarrow{k}_{-2}}{\overset{\overrightarrow{k}_2}{\rightleftharpoons}} \mathrm{M} + \mathrm{H_2} + \mathrm{M_{surface}}, \tag{7.50}$$

$$2\mathrm{MH_{ads}} \underset{k_{-3}}{\overset{k_3}{\rightleftharpoons}} 2\mathrm{M_{surface}} + H_2, \tag{7.51}$$

$$\mathrm{MH_{ads}} + \mathrm{M_{subsurface}} \underset{k_{-4}}{\overset{k_4}{\rightleftharpoons}} \mathrm{MH_{abs,0}} + \mathrm{M_{surface}}, \tag{7.52}$$

where $\mathrm{M_{surface}}$ and $\mathrm{M_{subsurface}}$ are the empty surface and subsurface sites. The absorbed hydrogen diffuses into the bulk [276]:

$$\mathrm{MH_{abs,0}} \rightleftarrows \mathrm{MH_{abs},}_x. \tag{7.53}$$

The rate of reaction (7.49) is described by Eq. (7.5) and that of reaction (7.52) by

$$v_4 = k_4\theta_\mathrm{H}(1 - X_0) - k_{-4}(1 - \theta_\mathrm{H})X_0, \tag{7.54}$$

where X is the dimensionless bulk hydrogen concentration, the surface concentration is $\mathrm{X_0} = C_{\mathrm{H},0}/C_{\mathrm{H,max}}$, and $C_{\mathrm{H,max}}$ is the saturation concentration under given experimental conditions. A thus defined X takes values between 0 and 1. Under steady-state conditions, when $v_4 = 0$, Eq. (7.54) becomes

$$X_0 = \frac{k_4\theta_{\mathrm{H}}}{k_4\theta_{\mathrm{H}} + k_{-4}(1-\theta_{\mathrm{H}})} = \frac{K_4\theta_{\mathrm{H}}}{K_4\theta_{\mathrm{H}} + (1-\theta_{\mathrm{H}})}, \tag{7.55}$$

which defines the absorption isotherm and $K_4 = k_4/k_{-4}$ is the absorption equilibrium constant. The diffusion of hydrogen into metal is described by Fick's equation:

$$\frac{\partial X}{\partial t} = D_{\mathrm{H}} \frac{\partial^2 X}{\partial x^2}, \tag{7.56}$$

and the surface hydrogen flux equals the absorption rate:

$$J_{\mathrm{H}} = -D_{\mathrm{H}} \frac{\sigma_{\mathrm{X}}}{F} \left(\frac{\partial X}{\partial x} \right)_{x=0} = v_4, \tag{7.57}$$

where $\sigma_{\mathrm{X}} = FC_{\mathrm{H,max}}$ is the charge corresponding to the saturation of metal with hydrogen.

Diffusion Eq. (7.56) must be solved for the oscillating dimensionless concentration of hydrogen: $\Delta X = \widetilde{X}\exp(j\omega t)$, and an equation analogous to (4.22) is obtained:

$$j\omega\widetilde{X} = D_{\mathrm{H}} \frac{\mathrm{d}^2\widetilde{X}}{\mathrm{d}x^2}, \tag{7.58}$$

and, assuming finite-length linear diffusion with the impermeable conditions at $x = l$,

$$\begin{aligned} x = 0 \quad & -D_{\mathrm{H}} \frac{\sigma_{\mathrm{X}}}{F} \frac{\mathrm{d}\widetilde{X}}{\mathrm{d}x} = \widetilde{J}_{\mathrm{H}}, \\ x = l \quad & \frac{\mathrm{d}\widetilde{X}}{\mathrm{d}x} = 0. \end{aligned} \tag{7.59}$$

The solution of Eq. (7.58) is

$$\widetilde{X} = A\mathrm{e}^{-sx} + B\mathrm{e}^{sx}, \tag{7.60}$$

where $s = \sqrt{j\omega/D_{\mathrm{H}}}$. Taking into account the boundary conditions, the solution for $\widetilde{X}$ is

$$\widetilde{X} = \frac{F}{\sigma_{\mathrm{X}}} \frac{\widetilde{J}_{\mathrm{H}}}{\sqrt{j\omega D_{\mathrm{H}}}} \frac{\cosh[s(l-x)]}{\sinh[sl]}, \tag{7.61}$$

and at the electrode surface

$$\widetilde{X}_0 = \frac{F}{\sigma_X}\frac{\widetilde{J}_H}{\sqrt{j\omega D_H}}\coth\left(\sqrt{\frac{j\omega}{D_H}}\, l\right). \tag{7.62}$$

From Eq. (7.62) the hydrogen flux is

$$\widetilde{J}_H = \frac{\sigma_X}{F}\widetilde{X}_0\sqrt{j\omega D_H}\,\tanh\left(\sqrt{\frac{j\omega}{D_H}}l\right) = J_H^{'}\widetilde{X}_0 = \left(\frac{\partial v_4}{\partial \theta_B}\right)\widetilde{\theta}_B + \left(\frac{\partial v_4}{\partial X_0}\right)\widetilde{X}_0, \tag{7.63}$$

where

$$J_H^{'} = \frac{\sigma_X}{F}\sqrt{j\omega D_H}\,\tanh\left(\sqrt{\frac{j\omega}{D_H}}l\right). \tag{7.64}$$

The current is given by

$$-\frac{\Delta i}{F} = \Delta r_0 = \Delta v_1 + \Delta v_2 \tag{7.65}$$

and its phasor by

$$\widetilde{r}_0 = -\frac{\widetilde{i}}{F} = \left(\frac{\partial r_0}{\partial \eta}\right)\widetilde{\eta} + \left(\frac{\partial r_0}{\partial \theta_H}\right)\widetilde{\theta}_H. \tag{7.66}$$

A similar linearization must be applied to the surface coverage by adsorbed hydrogen:

$$\begin{aligned}\frac{\sigma_1}{F}\frac{d\widetilde{\theta}_H}{dt} &= \frac{\sigma_1}{F}j\omega\theta_H = \widetilde{v}_1 - \widetilde{v}_2 - 2\widetilde{v}_3 - \widetilde{v}_4 = \widetilde{r}_1 - \widetilde{v}_4 \\ &= \left(\frac{\partial r_1}{\partial \theta_H}\right)\widetilde{\theta}_H + \left(\frac{\partial r_1}{\partial \eta}\right)\widetilde{\eta} - \left(\frac{\partial r_4}{\partial \theta_H}\right)\widetilde{\theta}_H - \left(\frac{\partial r_4}{\partial X_0}\right)\widetilde{X}_0.\end{aligned} \tag{7.67}$$

This equation is simplified because $\partial r_1/\partial X_0 = \partial v_4/\partial \eta = 0$. Equations (7.63), (7.66), and (7.67) can be written in matrix form:

$$\begin{bmatrix} -\dfrac{\partial r_0}{\partial \eta} \\ -\dfrac{\partial r_1}{\partial \eta} \\ 0 \end{bmatrix} = \begin{bmatrix} -\dfrac{1}{F} & \dfrac{\partial r_0}{\partial \theta_H} & 0 \\ 0 & \dfrac{\partial r_1}{\partial \theta_H} - \dfrac{\partial v_4}{\partial \theta_H} - j\omega\dfrac{\sigma_1}{F} & -\dfrac{\partial v_4}{\partial X_0} \\ 0 & \dfrac{\partial v_4}{\partial \theta_H} & \dfrac{\partial v_4}{\partial X_0} - J_H^{'} \end{bmatrix} \begin{bmatrix} \dfrac{\widetilde{i}}{\widetilde{\eta}} \\ \dfrac{\widetilde{\theta}_H}{\widetilde{\eta}} \\ \dfrac{\widetilde{X}_0}{\widetilde{\eta}} \end{bmatrix}. \tag{7.68}$$

The solution obtained using Cramer's rule is $\widetilde{i}_f/\widetilde{\eta} = T_1/B$:

$$T_1 = \begin{vmatrix} -\dfrac{\partial r_0}{\partial \eta} & \dfrac{\partial r_0}{\partial \theta_{\mathrm{H}}} & 0 \\ -\dfrac{\partial r_1}{\partial \eta} & \dfrac{\partial r_1}{\partial \theta_{\mathrm{H}}} - \dfrac{\partial v_4}{\partial \theta_{\mathrm{H}}} - j\omega\dfrac{\sigma_1}{F} & -\dfrac{\partial v_4}{\partial X_0} \\ 0 & \dfrac{\partial v_4}{\partial \theta_{\mathrm{H}}} & \dfrac{\partial v_4}{\partial X_0} - J_{\mathrm{H}}^{'} \end{vmatrix} \tag{7.69}$$

and

$$B = \begin{vmatrix} -\dfrac{1}{F} & \dfrac{\partial \partial r_0}{\partial \theta_{\mathrm{H}}} & 0 \\ 0 & \dfrac{\partial r_1}{\partial \theta_{\mathrm{H}}} - \dfrac{\partial v_4}{\partial \theta_{\mathrm{H}}} - j\omega\dfrac{\sigma_1}{F} & -\dfrac{\partial v_4}{\partial X_0} \\ 0 & \dfrac{\partial v_4}{\partial \theta_{\mathrm{H}}} & \dfrac{\partial v_4}{\partial X_0} - J_{\mathrm{H}}^{'} \end{vmatrix}, \tag{7.70}$$

from which the faradaic admittance is

$$\hat{Y}_{\mathrm{f}} = -\frac{\widetilde{i}}{\widetilde{\eta}} = -F\left(\frac{\partial r_0}{\partial \eta}\right) - \frac{\dfrac{F^2}{\sigma_1}\left(\dfrac{\partial r_0}{\partial \theta_{\mathrm{H}}}\right)\left(\dfrac{\partial r_1}{\partial \eta}\right)}{j\omega - \dfrac{F}{\sigma_1}\left(\dfrac{\partial r_1}{\partial \theta_{\mathrm{H}}}\right) + \dfrac{\dfrac{F}{\sigma_1}\left(\dfrac{\partial v_4}{\partial \theta_{\mathrm{H}}}\right)}{1 - \dfrac{\left(\dfrac{\partial v_4}{\partial X_0}\right)}{J_{\mathrm{H}}^{'}}}}, \tag{7.71}$$

which may written in a form similar to Eq. (5.51) for an electrocatalytic reaction with one adsorbed species and to that for the HER:

$$\widetilde{Y}_f = A + \frac{B}{j\omega + C + \dfrac{D}{1 + \dfrac{E}{\sqrt{j\omega D_{\mathrm{H}}}\tanh\left(\sqrt{\frac{j\omega}{D_{\mathrm{H}}}}l\right)}}}, \tag{7.72}$$

where the parameters A, B, and C are as defined earlier, Eq. (5.52), and D and E are defined as

$$D = \frac{F}{\sigma_1}\left(\frac{\partial v_4}{\partial \theta_{\mathrm{H}}}\right)_{X_0} \text{ and } E = -\frac{F}{\sigma_{\mathrm{X}}}\left(\frac{\partial v_4}{\partial X_0}\right)_{\theta_{\mathrm{H}}}. \tag{7.73}$$

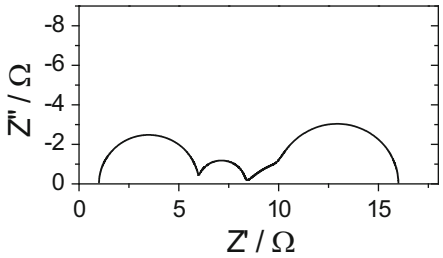

Fig. 7.6 Complex plane plot corresponding to hydrogen evolution and adsorption in finite-length reflective conditions; $R_s = 1\ \Omega$, $C_{dl} = 20\ \mu F$, $C_p = 0.01$ F, $R_{ct} = 5\ \Omega$, $R_p = 10\ \Omega$, $R_{ab} = 3\ \Omega$, $R_D = 10\ \Omega$, $T_D = 1{,}000$ s, see Eq. (4.77) for definition of latter two parameters

The difference between Eqs. (5.51) and (7.72) is the presence of the additional term in the denominator. The faradaic impedance is

$$\begin{aligned}\hat{Z}_f &= \frac{1}{\hat{Y}_f} \\ &= \frac{1}{A} - \frac{1}{j\omega\left(\frac{A^2}{B}\right) + \left(\frac{A^2C}{B} + A\right) + \frac{1}{\left(\frac{B}{A^2D}\right) + \left(\frac{BE}{A^2D}\right)\frac{\coth\left(\sqrt{\frac{j\omega}{D_H}}l\right)}{\sqrt{j\omega D_H}}}} = \\ &= R_{ct} + \frac{1}{j\omega C_p + \frac{1}{R_p} + \frac{1}{R_{ab} + \hat{Z}_W}},\end{aligned} \tag{7.74}$$

where R_{ct}, R_p, and C_p are as defined in Eq. (5.55) and the new parameters are

$$\begin{aligned}R_{ab} &= -\frac{B}{A^2D} = \frac{1}{C_p}\frac{1}{D}; \qquad \sigma' = -\frac{BE}{A^2D} = \frac{1}{C_p}\frac{E}{D}; \\ \hat{Z}_W &= \frac{\sigma'}{\sqrt{j\omega D_H}}\coth\left(\sqrt{\frac{j\omega}{D_H}}l\right).\end{aligned} \tag{7.75}$$

This equation corresponds to a circuit similar to that in Fig. 7.4 (where R_{ab} replaces R_d). The complex plane plot corresponding to the total circuit including the solution resistance and the double-layer capacitance is shown in Fig. 7.6. Three semicircles are observed corresponding to the coupling $R_{ct} - C_{dl}$, $R_{ab} - C_p$, and

$R_p - C_p$ and a part of the mass transfer impedance. In this case, the low-frequency impedance is real because a constant current flows through $R_s - R_{ct} - R_p$.

A case of finite diffusion length with transmissive boundary conditions has also been considered in the literature [277, 278]. It corresponds to the case where hydrogen diffuses across a membrane and is oxidized on the other side. The same Eq. (7.74) is obtained but with tanh replacing coth in Eq. (7.75).

7.4.2 Direct Hydrogen Absorption and Hydrogen Evolution

Most authors assumed the foregoing indirect adsorption–absorption mechanism; however, others proposed a direct absorption mechanism [279–281]:

$$M_{subsurface} + H^+ + e \underset{\overleftarrow{k}_5}{\overset{\overrightarrow{k}_5}{\rightleftharpoons}} MH_{abs,0}, \tag{7.76}$$

with the rate

$$v_5 = \overrightarrow{k}_5(1 - X_0) - \overleftarrow{k}_{-5}X_0, \tag{7.77}$$

from which the subsurface hydrogen concentration is

$$X_0 = \frac{\overline{K}_5}{1 + \overline{K}_5} \text{ and } \overline{K}_5 = \frac{\overrightarrow{k}_5}{\overleftarrow{k}_{-5}} = \frac{k_5^0}{k_{-5}^0} e^{-f\eta}. \tag{7.78}$$

This reaction leads to an impedance, $\hat{Z}_{abs}$, consisting of the charge transfer resistance and mass transfer impedance:

$$\hat{Z}_{abs} = R_{ct,abs} + \hat{Z}_W, \tag{7.79}$$

where

$$\begin{aligned} \frac{1}{R_{ct,abs}} &= A = -F\left(\frac{\partial v_5}{\partial \eta}\right)_{X_0}, \\ \hat{Z}_W &= \frac{\sigma'}{\sqrt{j\omega D_H}} \coth\left(\sqrt{\frac{j\omega}{D_H}}\, l\right), \\ \sigma' &= \frac{E}{A}, E = -\frac{F}{\sigma_X}\left(\frac{\partial v_6}{\partial X_0}\right), \end{aligned} \tag{7.80}$$

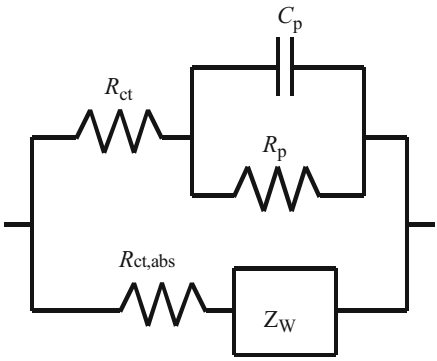

Fig. 7.7 Electrical equivalent circuit for faradaic impedance of direct hydrogen absorption in presence of hydrogen adsorption–evolution

and the mass transfer impedance was written for the finite-length reflecting conditions. Of course, besides the hydrogen direct absorption, hydrogen adsorption and evolution might take place. The total electrical equivalent circuit for the faradaic impedance is displayed in Fig. 7.7, where the upper branch corresponds to hydrogen adsorption and evolution and the lower branch corresponds to direct hydrogen absorption.

Besides hydrogen evolution and absorption, there might also be a HUPD reaction adding another R_{UPD}-C_{UPD} branch in parallel [272, 282]. From a structural point of view circuits for indirect and direct hydrogen absorption are indistinguishable. Studies of hydrogen absorption in palladium suggest that direct hydrogen absorption is faster than the indirect path [283, 284].

7.4.3 *Hydrogen Absorption in Absence of Hydrogen Evolution*

Very often hydrogen absorption is studied at potentials before hydrogen evolution, especially in the HUPD zone [282–285]. In such cases, the circuit becomes simplified because $R_p = \infty$ and parameter $B = -AC$. The faradaic impedance in the case of indirect adsorption–absorption mechanism becomes

$$\hat{Z}_f = R_{ct} + \frac{1}{j\omega C_p + \frac{1}{R_{ab} + \hat{Z}_W}}, \tag{7.81}$$

where

$$\begin{aligned} C_p &= \frac{A}{C} = f\sigma_1 \frac{\overline{K}_1}{\left(\overline{K}_1 + 1\right)^2}; R_{ab} = \frac{1}{C_p D}; \\ \sigma' &= \frac{E}{C_p D} = \frac{1}{f\sigma_X} \frac{\left(\overline{K}_1 K_4 + 1\right)^2}{\overline{K}_1 K_4}, \end{aligned} \tag{7.82}$$

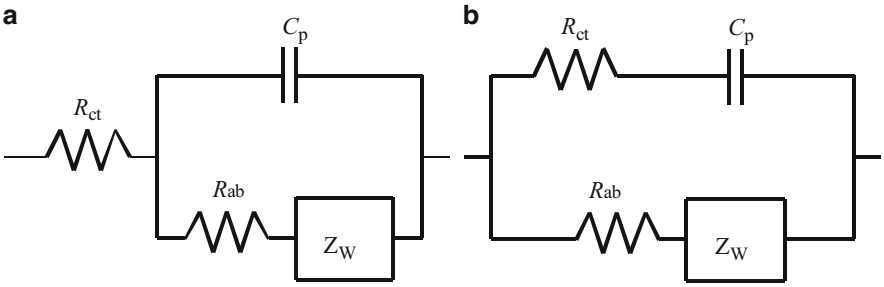

Fig. 7.8 Electrical equivalent circuits of faradaic impedance corresponding to (**a**) indirect, Eq. (7.81), and (**b**) direct, Eq. (7.83), hydrogen absorption reaction with finite-length linear diffusion of hydrogen

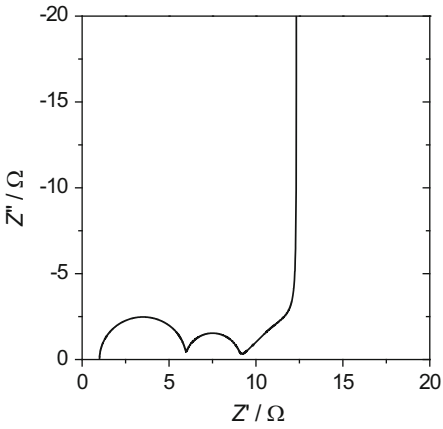

Fig. 7.9 Complex plane plot corresponding to indirect hydrogen absorption reaction, Eq. (7.81), in presence of finite-length reflective linear diffusion. Parameters: $R_s = 1\ \Omega$, $C_{dl} = 20\ \mu F$, $R_{ct} = 5\ \Omega$, $R_{ab} = 3\ \Omega$, $C_p = 0.01$ F, $R_D = 10\ \Omega$, $T_D = 1{,}000$ s

and for the direct absorption mechanism

$$\hat{Z}_f = \frac{1}{\frac{1}{R_{ct} + \frac{1}{j\omega C_p}} + \frac{1}{R_{ab} + \hat{Z}_W}}. \tag{7.83}$$

The electrical equivalent circuits of the faradaic impedance corresponding to the indirect, Eq. (7.81). and direct, Eq. (7.83), hydrogen absorption reaction with finite-length linear diffusion are displayed in Fig. 7.8.

The total impedance complex plane plot for indirect hydrogen absorption without hydrogen evolution, including solution resistance and double-layer capacitance, is displayed in Fig. 7.9. It shows two semicircles due to the $R_{ct} - C_{dl}$ and $R_{ab} - C_p$ coupling followed by the finite-length reflective linear diffusion displaying a line at 45° followed by a capacitive line at 90°.

In practice, the hydrogen absorption resistance is usually very small, and one semicircle is observed on the complex plane plots. Examples of the complex plane

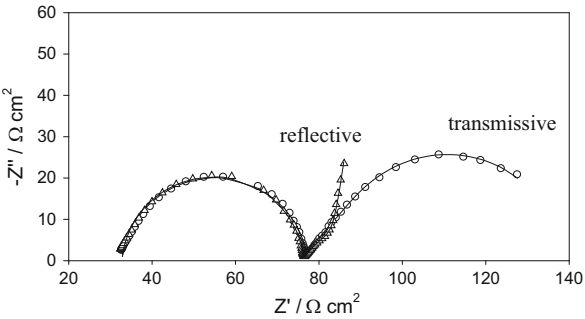

Fig. 7.10 Complex plane plots obtained on Pd foil (50 μm) in 0.1 M H_2SO_4 at $E = 0.12$ V versus reversible hydrogen electrode, RHE (From Ref. [286] with permission of author)

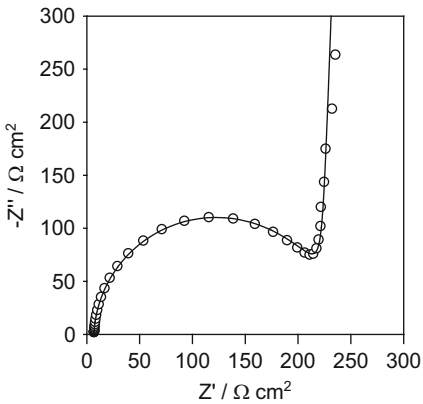

Fig. 7.11 Complex plane plots obtained on 10 ML of Pd on Au(111), in 0.1 M H_2SO_4 at $E = 0.15$ V versus RHE (From Ref. [286] with permission of author)

plots obtained for hydrogen absorption at Pd membrane in the transmissive and reflective conditions [155] are displayed in Fig. 7.10. The high-frequency part corresponding to the coupling $R_{ct} - C_{dl}$ is identical, and parts of the transmissive and reflective mass transfer impedances are visible (compare with Fig. 4.12).

For thin absorbing layers the mass transfer impedance in reflective conditions reduces to an $R_W - C_W$ connection in series, Eq. (4.85). The observed impedance for the hydrogen absorption reaction in 10 monolayers (ML) of Pd on Au(111) [155] is shown in Fig. 7.11, where a high-frequency semicircle is followed directly by a low-frequency vertical capacitive line (corresponding to the penetration of the ac signal to the bottom of the layer).

7.4.4 Hydrogen Absorption in Spherical Particles

Very often H absorption is studied in practical powdered materials (e.g., in NiMH batteries) that consist of spherical particles for which a finite-length spherical diffusion treatment must be used [287–289]. In this case the diffusion Eq. (7.56) must be written for the spherical diffusion, as in Eq. (4.91):

$$\frac{\partial X}{\partial t} = D_{\mathrm{H}} \left[\frac{\partial^2 X}{\partial r^2} + \frac{2}{r} \frac{\partial X}{\partial r} \right]. \tag{7.84}$$

Proceeding as in Sect. 4.6.2, the mass transfer impedance is described as

$$\hat{Z}_{\mathrm{W}} = \frac{\sigma' r_0}{D_{\mathrm{H}}} \frac{1}{\left[\left(\sqrt{\frac{j\omega}{D_{\mathrm{H}}}} r_0 \right) \coth\left(\sqrt{\frac{j\omega}{D_{\mathrm{H}}}} r_0 \right) - 1 \right]}, \tag{7.85}$$

and the impedance is as in Fig. 4.15. At low frequencies a capacitive behavior, Eq. (4.107), is observed as the hydrogen can diffuse only to the sphere center. This equation was used in modeling the hydrogen absorbing materials [287, 288, 290]. The influence of self-stress on hydrogen absorption has also been studied [291–294].

The preceding theory may be extended to other intercalation reactions, e.g., in lithium batteries. It has also been extended to bilayers [295, 296].

7.5 Conclusions

Hydrogen adsorption, evolution, and absorption reactions were presented as examples of electrocatalytic reactions, i.e., involving adsorption at the electrode surface. The general rules of development of impedance equations involving first the dc description followed by linearization of the equations were used. The electrode processes involved adsorption and mass transfer either in solution or inside the electrode material. In a similar way, other electrocatalytic reaction mechanisms such as, for example, oxygen reduction or evolution, chlorine evolution, and lithium intercalation, might be discussed. The transfer mechanisms of hydrogen through membranes might also be studied using transfer functions other than impedance and admittance; see, e.g., Ref. [61].